Electrophoretic mobilization in capillary isoelectric focusing by a weak acid or an acidic ampholyte as catholyte assessed by computer simulation

Wolfgang Thormann*

Institute for Infectious Diseases, University of Bern, Bern, Switzerland.

ORCID Wolfgang Thormann: https://orcid.org/0000-0002-9762-1609

Key words: capillary isoelectric focusing, computer simulation, electrophoretic mobilization, chemical mobilization

Abbreviations: ARG, arginine; ASP, aspartic acid; GLU, glutamic acid; IDA, iminodiacetic acid; SERO, serotonin; TYRA, tyramine.

***) Correspondence:**

Prof. Dr. W. Thormann

Institute for Infectious Diseases, University of Bern

CH-3008 Bern, Switzerland

Received: 10 28, 2022; Revised: 11 19, 2022; Accepted: 11 26, 2022

This article has been accepted for publication and undergone full peer review but has not been through the copyediting, typesetting, pagination and proofreading process, which may lead to differences between this version and the Version of Record. Please cite this article as doi: 10.1002/elps.202200262.

E-Mail: wolfgang.thormann@unibe.ch

Abstract

CIEF with cationic electrophoretic mobilization induced via replacing the catholyte with the anolyte or a solution of another acid or amino acid was investigated by computer simulation for a wide range pH gradient bracketed between two amphoteric spacers and short electrode vials with a higher id than the capillary. Dynamic simulations provide insight into the complexity of the mobilizing process in a hitherto inaccessible way. The electrophoretic mobilizing process begins with the penetration of the mobilizing compound through the entire capillary, is followed by a gradual or steplike decrease of pH, and ends in an environment with a non-homogenous solution of the mobilizer. Analytes do not necessarily pass the point of detection in the order of decreasing pI values. Cationic mobilization encompasses an inherent zone dispersing and refocusing process towards the capillary end. This behavior is rather strong with phosphoric acid and citric acid, moderate with aspartic acid, glutamic acid, formic acid and acetic acid, and less pronounced in absence of the cathodic spacer. The data reveal that optical detectors should not be placed before 90 % of capillary length. Aspartic acid, glutamic acid, formic acid and acetic acid provide an environment with a continuously decreasing pH which explains their successful use in optimized two-step CIEF protocols.

1 Introduction

CIEF utilizes capillaries or microchannels as focusing columns and represents a high-resolution technique for separation and analysis of amphoteric molecules, mainly proteins, in a pH gradient which increases from anode to cathode. When CIEF is performed in quiescent solution, analyte visualization is possible via whole column imaging or a scanning detector. Alternatively, the sample pattern must be mobilized either during or following focusing such that analytes can be detected as they pass an on-column optical (absorbance or fluorescence) detector that is mounted towards one column end or as they are transported across the column end into the ionization interface of a MS or a flowing stream. Mobilization in CIEF can be

accomplished by electrophoretic means, imposed flow (via utilization of pressure, vacuum or gravity), electroosmosis or combinations of these principles [1-8].

CIEF with electrophoretic mobilization was first described by Hjertén's group and is typically performed as a two-step process [9,10]. Focusing is completed in quiescent solution and the focused ampholytes are then mobilized either toward the anode or toward the cathode. Anionic mobilization is accomplished by replacing the anolyte (typically an acid) by a base or by putting salt into the anolyte (i.e. addition of a cation) and reapplication of power. Conversely, mobilization occurs towards the cathode when the catholyte (typically a base) is replaced by an acid or a solution of the base containing a salt (addition of an anion). In the scientific literature, these principles are also referred to as chemical or salt mobilization [1-10].

For many years, one-dimensional dynamic models have been developed for electrophoresis and computer simulations were conducted to understand the fundamentals and phenomena of electrophoretic processes, including those of CIEF. One of these models, GENTRANS, was extensively used to describe the separation dynamics of sample and ampholyte compounds in CIEF, the formation, stability and decomposition of the pH gradient, sampling strategies with sequential injection of sample and carrier ampholytes and conditions that lead to the formation or prevention of a pure water zone at pH 7 (for reviews refer to [11-13]). Selected aspects of mobilization in CIEF, namely electrophoretic salt mobilization after focusing [14], focusing with concurrent electrophoretic mobilization [15,16,17], and mobilization based on EOF [17,18] were also studied. Furthermore, a non-released developer version of SIMUL5 [19] was employed to gain qualitative insight into the behavior of different chemical mobilization schemes in microchip IEF systems comprising 10 carrier ampholytes [20]. This unreleased version of the simulator from the Gaš group includes closed boundary conditions at column ends in a column divided into an array of compartments with identical or different cross sections in which the solutions are mixed. It permitted to mimic the well reservoirs with varying capillary cross-sections used in microchip IEF [20] and led to the simulation of isoelectric trapping separations and desalting that take place in recirculating multicompartmental electrolyzers [21].

The recently released SIMUL6 simulator, the successor of SIMUL5, comprises a completely new source code that leads to faster procedures for the numerical integration of partial

differential equations and uses multithreaded computation [22]. This made the simulator up to 15 times faster compared to SIMUL5. SIMUL6 features two options that are important to accurately simulate electrophoretic mobilization in IEF under constant voltage conditions in both CIEF and microchip IEF. First, the separation column can be divided into a number of individual sections and the diameter of each section can be set individually. In all segments, transversal diffusion is assumed to be infinitely fast which represents a quasi 1D approach that was used previously in other models [21,23,24]. Having larger diameters at the column ends permits the simulation of the impact of electrode compartments and provides a configuration that is typically employed in experiments. Second, swapping of a part of the electrolyte with another electrolyte during the run is required to study electrophoretic mobilization in IEF [14]. These aspects, together with user friendly interfaces for data input, online data visualization during simulation and data export, makes SIMUL6 an ideal tool to study IEF systems with a large number of components [13,22].

In the early work of Hjertén et al. [1,9,10] electrophoretic mobilization is explained via the gradual ion penetration from the electrode chamber through the gradient thereby causing a change of the charge status of each ampholyte. This principle could be verified by computer simulation for the case of salt mobilization and thereby shown to occur isotachophoretically [14]. Prior to the availability of SIMUL6, anionic mobilization by replacing the anolyte with the catholyte and cationic mobilization by replacing the catholyte with anolyte was only simulated for two simple systems using a low number of ampholytes [19]. SIMUL6 [22] provides an IEF example with a wide pH range featuring 182 model carrier ampholytes, 14 fully characterized amphoteric analytes from the literature [25] and two amphoteric spacer compounds as sample, H_3PO_4 as anolyte and LiOH as catholyte. This example was used to elucidate the details of cathodic electrophoretic mobilization with various acidic compounds as mobilizers, including acetic acid employed in typical two-step CIEF protocols with optical analyte detection [26,27,28,29], formic acid applied in CIEF-MS [30,31] and glutamic acid (GLU) for high resolution in the pI 4 to 5 range [29]. Simulations were performed with SIMUL6 under realistic conditions using constant voltage and short electrode vials with larger diameters compared to that of the capillary as is customary in experiments. This study provides insights that were hitherto inaccessible and are complementary to experimental findings, including those reported by Zhu et al. [32] and Manabe et al. [33]. Detailed

simulation data of two-step CIEF using weak acids and acidic amino acids as catholytes for cationic electrophoretic mobilization are presented here for the first time.

2 Materials and Methods

2.1 Computer simulation program

SIMUL6 [22] can be downloaded from https://echmet.natur.cuni.cz and https://www.simul6.app. SIMUL6 has a user-friendly interface to input all parameters and simulations in progress can be followed graphically on frames that show the distributions of all components, pH, conductivity and the electric field strength along the column, the current and voltage as function of time, and the signal of a detector placed at a selected position along the column. SIMUL6 comprises a feature to divide the column into a number of individual sections and the diameter of each section can be set individually. Having larger diameters at the column ends permits the simulation of the impact of electrode compartments in IEF. Furthermore, the provided swapping of a part of the solution with another electrolyte at a specified time interval allows the study of electrophoretic mobilization in IEF in a more convenient way compared to that offered with GENTRANS [14]. SIMUL6 version 1.4 was employed for all simulations.

2.2 Input conditions and execution of simulations

The configuration presented as IEF example in Refs. [13,22] was used in this work. If not stated otherwise, a 50 µm id capillary of 54 mm length was placed between circular electrode vials of 5000 µm id and 9 mm length. Focusing of 14 amphoteric analytes (0.01 mM each) in a mixture with 182 carrier ampholytes (0.1 mM each) and two spacing components (10.5 mM iminodiacetic acid (IDA) and 8.79 mM arginine (ARG)) was simulated. 300 mM H_3PO_4 (anolyte, between 0 and 9 mm of column) and 200 mM LiOH (catholyte, between 63 and 72 mm of column length) served as electrode solutions for focusing. The entire column of 72 mm length was divided into 1000 segments of equal length and the zone edge was set to 1 mm. Focusing occurred during 3000 s at a constant 100 V. Thereafter, the cathodic electrode solution was replaced with the anolyte (300 mM H_3PO_4) or another 300 mM solution of a mobilizer and electrophoretic mobilization was induced by a continuation of power application (100 V) for 4200 to 8000 s. The carrier ampholytes were assumed to be monovalent components with ΔpKa equal to 1. The pI's of the carrier ampholytes ranged between 3.00 and 10.30 and were uniformly distributed. The cationic and anionic mobilities

of all carrier ampholytes were set to 20×10^{-9} m^2/Vs. The input data of the 14 analytes with pI values from 2.99 to 10.58 represent real values and are those provided in [25]. Mobility and pKa values of ARG and the compounds in the electrode vials were taken from the data base of SIMUL6. The values for IDA were those provided in the simulation example of SIMUL6. The detector position was at 57.6 mm that corresponds to 90% of the focusing capillary length. SIMUL6 was executed with parallel computing, optimized time stepping and the maximum error set to 10^{-7} on a 64bit Windows 10 based PC featuring an Intel Core I7-10700K processor (8 cores, 16 threads) running at 3.8 GHz. For making plots, data were imported into the SigmaPlot Scientific Graphing Software Windows Version 12.5 (SPSS, Chicago, IL, USA).

3 Results and discussion

3.1 Focusing example

The focusing of 14 amphoteric analytes together with 182 carrier ampholytes and two spacing components between 300 mM H_3PO_4 as anolyte (between 0 and 9 mm of column length) and 200 mM LiOH as catholyte (between 63 and 72 mm of column length) are presented in Figure 1. Distributions of all components, the analytes together with IDA and ARG, anolyte and catholyte together with IDA and ARG, as well as pH, conductivity and the electric field strength are presented in different panels (from bottom to top, respectively). The presented data are those obtained after application of a constant 100 V for 3000 s for a configuration with electrode vials of 5000 µm id (Figure 1A) and 50 µm id (Figure 1B).

In both cases, IDA (pI 2.33) is focused between the anolyte and the anodic end of the carrier ampholytes whereas ARG (pI 11.36) between the catholyte and the cathodic end of the carrier ampholytes (bottom panels in Figure 1). The focused spacers are contracting the carrier ampholytes and thus the established pH gradient within the capillary to a length of about 35 mm (instead of the 54 mm in absence of these compounds, data not shown). They are necessary for the detection of all analytes with single detectors placed towards the column ends, i.e. outside the focused analytes. This is nicely shown with the data presented in Figure 1. The two spacing compounds IDA and ARG are used in many optimized CIEF protocols [25-31], including those developed for commercial kits. In earlier work with cathodic electrophoretic mobilization, TEMED instead of ARG was used as spacer [32]. Furthermore, in the case without an increase in the diameter of the electrode compartments (Figure 1B), the

spacing compounds penetrate somewhat further into the electrode vessels. IDA and ARG define early and late portions of the pH gradient and are not present within pH gradient established by the carrier ampholytes. For the situation with a 100-fold larger diameter of the electrode compartments (Figure 1A), a small part of the both spacing compounds becomes trapped in the electrode solutions which is seen in the second panel from bottom. As a consequence, small amounts become continuously released and travel through the gradient, ARG from the anodic side towards the cathode and IDA in the other direction. For the 3000 s time point presented in Figure 1A, the concentration of ARG and IDA within the carrier ampholyte gradient is predicted to be about 7.2 µM and 1.4 µM, respectively. Comparable data were obtained for focusing at 600 V and 500 s, with 3-4 times higher concentrations of ARG and IDA migrating within the carrier ampholytes. Application of 600 V is more realistic in terms of experimental work and provides sharper foci [13]. However, such simulations require a tighter mesh (6000 segments), take significantly more time to be completed (8.7 min vs. 304.9 min, respectively) and produce huge data files. Thus, all data presented in this paper were performed with 100 V and 1000 segments and, except for those of Figure 1B, the columns were assumed to have 9 mm electrode compartments with 5000 µm id.

Conductivity, pH and electric field distributions are presented in the top panels of Figure 1. Except for the edge regions, the pH increases linearly from 2.60 at the anodic end to 10.25 on the cathodic side. Most of the 14 amphoteric analytes focus within this gradient. Serotonin (SERO) with a pI value of 10.58 focuses within the ARG zone whereas tyramine (TYRA, pI of 10.17) and dansylated iminodiacetic acid (DNS-IDA, pI of 2.99) form their foci at the edges of ARG and IDA, respectively. With the employed input values, conductivity and electric field strength throughout the gradient are predicted to be uniform along a large part of the gradient. The electric field strength within the ARG zone is higher and the conductivity lower because ΔpKa of ARG is large (4.88, pKa values of 8.92 and 13.80) which makes it is less conductive. The opposite is true for IDA which has a low ΔpKa (1.02, pKa values of 1.82 and 2.84). Furthermore, the predicted currents as function of time for the 3000 s focusing time interval are given as inserts in the second panels from top.

3.2 Cationic mobilization with the anolyte as catholyte

After 3000 s of focusing (Figure 1A), the catholyte in the electrode vial was exchanged with the anolyte, namely 300 mM phosphoric acid which has pKa values of 2.16, 7.21 and 12.7 (bottom panel of Figure 2A) followed by reapplication of a constant 100 V. The data presented in Figure 2 reveal the expected gradual phosphate penetration from the cathodic electrode chamber through the gradient thereby causing a change of the charge status of each ampholyte and thus electrophoretic mobilization of all ampholytes towards the cathode. This is visualized with the distributions of all components obtained after 4000, 5000 and 6000 s (i.e. 1000, 2000 and 3000 s of mobilization) presented in Figure 2A (second, third and fourth panel from bottom, respectively). Lithium (from the original catholyte present within the cathodic capillary end after the buffer exchange, bottom panel of Figure 2A) and ARG are the first compounds that migrate into the cathodic electrode vial. The carrier ampholytes and the analytes are predicted to follow gradually. IDA becomes only slightly mobilized within the 3000 s of voltage reapplication. It is important to realize that the compounds become strongly diluted upon entering the cathodic electrode vial with a 1000-fold higher id and are thus not displayed on the y-scales used in the panels of Figure 2A. Furthermore, the current is increasing during mobilization at constant voltage. The currents for the four time points are 0.098, 0.220, 1.135 and 1.658 µA, respectively. The initial current increase is responsible for the tightening of carrier ampholytes seen in the 4000 s data (second panel from bottom). Later on, carrier ampholytes become spread out.

Distributions of phosphoric acid, electric field strength and pH at a 500 s interval during electrophoretic mobilization with phosphoric acid are presented in the top panels of Figure 2B. These profiles show the complexity of the property changes occurring during mobilization. The phosphoric acid concentration and the electric field strength along the IEF column are not uniform and change with time. The pH profile becomes gradually lower during the first 1000 s, then collapses within the second 1000 s of mobilization, and finally reaches an almost uniform distribution along the column. Of interest for cationic mobilization is the phosphoric acid concentration dip that develops between 48 and 60 mm of the column. There is an electric field strength peak associated with this dip such that the migrating amphoteric compounds become first broader while experiencing an increasing electric field strength and then become refocused at the cathodic end of the dip when the electric field decreases. For selected analytes, this behavior is illustrated with the 100 s interval data presented in the lower panels of Figure 2B. As a consequence of this behavior, a detector

should not be placed at a column position < 90% of the focusing capillary length, i.e. before 57.6 mm in the investigated example which is marked with the grey dashed line in all panels of Figure 2.

The predicted detector plot of all analytes for a detector placed at 57.6 mm is presented in the lower panel of Figure 3A. Also presented are the profiles for the spacer ARG (dark pink dashed line graph with y-scale on left side) and the mobilizing compound phosphoric acid (dark grey dashed line graph with y-axis scale on the right side). Furthermore, the upper panel depicts the associated profiles for pH (brown line graph) and conductivity (black line graph) at the location of the detector as function of time together with the temporal behavior of the current during mobilization (red line graph). These data reveal that peak shapes vary. The first two analytes (SERO as sharp peak and TYRA as broader peak) are detected within ARG and metanephrine (analyte 3) within the vanishing ARG boundary. Furthermore, there is a step increase of phosphoric acid and thus pH decrease at the same location.

During mobilization, the current increases with time (upper panel of Figure 3A). Responses of the analytes detected up to 2000 s of mobilization (5000 s of two-step procedure) are sharper at the time of detection compared to those thereafter. Detection of analytes occurs essentially in the order of decreasing pI values. However, there are two exceptions. 4-(4-aminophenyl) butyric acid (pI 4.86, analyte 10) is detected ahead of leucoberbelin blue I dye (pI 5.27, analyte 9) and 3-methylhistidine (pI 7.71, analyte 7) and glycyl-histidine (pI 7.55, analyte 8) are detected at the same time (Figure 3A). Furthermore, ARG trapped in the anodic electrode compartment, as is depicted in Fig. 1A, becomes continuously delivered towards the cathode during the entire mobilization period. After removal of the ARG spacer zone, the concentration of ARG decreases to a very low concentration around 5000 s. This is followed by a gradual ARG concentration increase after 5100 s and finally reaches a level of about 0.08 mM at 6000 s which is comparable to the peak concentration of the most acidic analyte (analyte 14 in Figure 3A).

3.3 The choice of the mobilizing compound

The detector data presented in panels B to F of Figure 3 were obtained with 5 mobilizers that were applied as catholyte instead of phosphoric acid and otherwise identical conditions as for panel A of Figure 3. Using citric acid (Figure 3B) with pKa values of 3.13, 4.76 and 6.40 revealed data that are similar to those of phosphoric acid (Figure 3A). There is again a

breakdown of the pH gradient with a step change at the end of ARG detection. The current and conductivity are lower compared to the case with phosphoric acid and detection times are somewhat higher.

Employing 300 mM GLU as catholyte in the mobilizing step resulted in the data depicted in Figure 3C. This system is characterized with a much lower current, a lower conductivity and a gradual pH decrease from around 10.5 to about 3.4. Compared to the cases of panels A and B, the entire mobilizing process occurs in a smoother way, the migration velocities of the mobilized analytes are lower, and most peaks are predicted to be higher and of comparable shape. The data presented in Figure 4A illustrate that there is no rapid collapse of the pH gradient and that the electric field strength distribution remains uniform over a large part of the column. The dip of the mobilizing compound in the 48 to 60 mm column region develops as well but has a lower impact on the electric field strength change and thus dispersion of analyte distribution compared to the case with phosphoric acid or citric acid as mobilizing compounds. However, mobilization with GLU has a limited applicability in terms of analytes with acidic pIs. Analytes with pI values < 4.20 migrate very slowly and become dispersed such that they are essentially lost for detection (Figure 4A). This was assessed with a run time up to 10000 s during which DNS-GLU was detected as broad peak between 9000 and 10000 s and DNS-aspartic acid (ASP) as well as DNS-IDA were not detected (data not shown). This limitation was previously discussed in the context of experimental work [28,32]. Detection of analytes occurs essentially in the order of decreasing pI values. This is also true for leucoberbelin blue I dye (pI 5.27, analyte 9) and 4-(4-aminophenyl) butyric acid (pI 4.86, analyte 10). Furthermore, glycyl-histidine (pI 7.55, analyte 8) and 3-methylhistidine (pI 7.71, analyte 7) are detected separately but not in the order of decreasing pI values.

Using ASP as mobilizing agent instead of GLU induced a comparable cationic mobilization (data not shown). Detection times were somewhat shorter with the detection time of DNS-GABA shortly after 6000 s. DNS-GLU and DNS-ASP were monitored as broad peaks shortly before 7000 and 8000 s, respectively. DNS-IDA did not reach the detector within 10000 s. Thus, ASP instead of GLU provides a somewhat elongated range for the detection of analytes with low pI values (data not shown). Furthermore, using IDA as mobilizer resulted in data very similar to those of chloroacetic acid presented in Figure 3D in which leucoberbelin blue

I dye (pI 5.27, analyte 9) and 4-(4-aminophenyl) butyric acid (pI 4.86, analyte 10) are predicted to be detected together. Thus, IDA is not an ideal mobilizer.

The data presented in panels D to F of Figure 3 were obtained with monovalent weak acids as mobilizing compounds. Using 300 mM chloroacetic acid (pKa of 2.86, mobility of 43.7 x $10^{-9}m^2/Vs$) provided the data of Figure 3D. Mobilization can be induced as quickly as with phosphoric acid (compare data of panel D with those of panel A), the pH drops without a sudden change and the detection order is the same as with GLU. Similar data were obtained with catholytes comprising 300 mM formic acid (pKa of 3.75, mobility of 56.6 x $10^{-9}m^2/Vs$, Figure 3E) and 300 mM lactic acid (pKa of 3.86, mobility of 36.5 x $10^{-9}m^2/Vs$; data not shown). Compared to the system with chloroacetic acid, simulation revealed more slowly migrating analytes and thus a better resolution, and better peaks for DNS-GLU (pI 3.49) and DNS-ASP (pI 3.34) as is shown with the data presented in Figure 3E. Furthermore, application of 300 mM acetic acid (pKa of 4.76, mobility of 42.4 x $10^{-9}m^2/Vs$) resulted in a high-resolution electropherogram (Figure 3F). In this system, the current is almost uniform and comparable to that with GLU. The migration velocities of the analytes are lower than those predicted with acids whose pKa values are lower. This is particularly well documented with ampholytes whose pI values are smaller than 9.0.

The distributions of pH and electric field strength are similar to those predicted with GLU as mobilizing agent. Analyte dispersion in the 48 to 60 mm column region is also present in these systems as is documented with the data for formic acid depicted in Figure 4B. However, its magnitude is smaller compared to that of phosphoric acid (compare data of Figure 4B with those of Figure 2B). With all the weak acids investigated in this work, cationic mobilization resulted in sharp detector signals for analytes down to pI 4.20. For lower pI values, predicted peak shapes are broader. This is associated with a strong increase of the concentration of the mobilizing compounds. In all cases with weak acids as mobilizing compounds, the order of analyte detection is the same as with GLU and ASP. In the systems studied, ARG delivered from the anode compartment is detected at a lower concentration compared to the case with phosphoric acid as mobilizing compound. Lowest concentrations are predicted for GLU and acetic acid (about 7 µM each; Figure 3C and 3F). Corresponding values for ASP and formic acid are about 10 µM and 25 µM, respectively.

Finally, it is interesting to note that the removal of residual Li and ARG occurred in about the same time interval in all investigated cases, and that DNS-IDA with a pI value of 2.99 cannot be detected efficiently by cationic mobilization having acids and acidic amino acids as mobilizing agents. All these data illustrate that phosphoric acid and citric acid should not be used. The simulation data reveal that GLU, ASP, formic acid and acetic acid are favorable compounds for cathodic electrophoretic mobilization.

3.4 The impact of the cathodic spacer compound on mobilization

IDA and ARG are spacing ampholytes that are added to the sample [22,25,26-31]. IDA is more acidic and ARG is more basic than any of the carrier ampholytes. They occupy the terminal regions of the IEF capillary (Figure 1), avoid the loss of carrier and sample ampholytes and, upon mobilization, permit detection of analytes that focus close to the end of the pH gradient. For cathodic electrophoretic mobilization, the role of ARG was investigated together with 300 mM phosphoric acid as mobilizer. With the given ARG concentration (8.79 mM), all basic analytes can be detected with the detector positioned at 90 % (57.6 mm) of the IEF column length (Figure 3A). With half the amount of ARG in the sample (4.395 mM), SERO focuses within the ARG zone at a more cathodic position than the selected detector and TYRA around the detector (data not shown). Thus, both analytes are lost for detection with cationic mobilization. Without ARG in the sample, SERO, TYRA and metanephrine cannot be monitored via cationic mobilization. Similarly, application of 8.79 mM LYS (pI 9.96) instead of ARG (pI 11.36) as spacing ampholyte on the cathodic side, SERO, TYRA and a number of basic carrier ampholytes are lost during focusing and thus for subsequent detection as the pI of LYS is lower than the pIs of these compounds (data not shown).

The impact of the cathodic spacer compound on the low conductivity region formed during cathodic electrophoretic mobilization was investigated via property changes of the spacer and employing 300 mM phosphoric acid as mobilizer. First, ΔpKa of ARG was set to unity (pKa values of 10.86 and 11.86) instead of 4.88 (pKa values of 8.92 and 13.80), a change that does not affect the pI value. Simulation revealed mobilization data that were essentially identical (data not shown). The use of LYS with its lower pI value than that of ARG (9.96 instead of 11.36) provided similar data as well. Finally, in absence of ARG, the analyte dispersion was somewhat less pronounced but still significant (Figure 5A, compare data with Figure 2B). The same phenomenon was observed with 300 mM formic acid as mobilizer. Removal of

ARG significantly reduced the effect of the low conductivity zone (Figure 5B, compare data with Figure 4B). These data suggest that sample dispersion in the cathodic part of the IEF column followed by refocusing towards the end of the focusing column is an inherent electrophoretic process. The magnitude of the effect is dependent on the presence of the spacer and the properties of the mobilizing compound. It is more pronounced with phosphoric acid and citric acid than with GLU, ASP, formic acid and acetic acid.

4 Concluding remarks

CIEF with cationic mobilization induced via replacing the catholyte with the anolyte or a solution of another acid or amino acid was investigated by computer simulation for a typical wide pH range system with IDA and ARG as amphoteric spacer compounds. The configuration encompassed short electrode vials with a higher id than the capillary and mobilization was induced via application of constant voltage. It reflects a typical setup used in two-step IEF protocols. The data reveal that phosphoric acid, citric acid, as well as monovalent acids with pKa values lower than about 3.5 are not ideal mobilizing compounds. Instead, ASP, GLU, formic acid and acetic acid are favorable mobilizers that provide an environment with a continuously decreasing pH. The electrophoretic mobilizing process is shown to be complex. It begins with the penetration of the mobilizing compound through the entire capillary, is followed by a gradual or steplike decrease of pH, and ends in an environment with a non-homogenous solution of the mobilizer. Although analytes are separated in carrier ampholyte based CIEF according to their pI, electrophoretic mobilization with a catholyte comprising a solution of a weak acid or an acidic amino acid can change the detection sequence of amphoteric analytes, i.e. the analytes do not necessarily pass the point of detection in the order of decreasing pI values.

Cationic electrophoretic mobilization of analytes is characterized with an inherent zone dispersion and refocusing process towards the cathodic capillary end. This behavior is rather strong with phosphoric acid and citric acid as mobilizing agents and more moderate with ASP, GLU, formic acid and acetic acid. Furthermore, simulation data revealed that in all cases the dispersing effect is less pronounced in absence of the spacer compound. For optimized detection sensitivity, on-line optical detectors should not be placed before 90 % of column length. The simulations performed with SIMUL6 provide insight into the complexity of the mobilizing process in a hitherto inaccessible way and confirm and underline the

successful use of GLU, formic acid and acetic acid reported for optimized CIEF configurations with cathodic electrophoretic mobilization [26-33]. It is important to note that cationic mobilization with an acid or an acidic amino acid added to the catholyte is not described here. Simulations of this topic have been reported previously [14,20].

Conflict of interest

The author has declared no conflict of interest.

Data availability statement

The data that support the findings of this study are available from the corresponding author upon reasonable request.

5 References

[1] Hjertén S. Isoelectric focusing in capillaries. In Grossman PD, Colburn JC, editors. Capillary electrophoresis, theory and practice. San Diego: Academic Press; 1992, p. 191-214.
[2] Pritchett TJ. Capillary isoelectric focusing of proteins. Electrophoresis. 1996;17:1195-201.
[3] Rodriguez-Diaz R, Wehr T, Zhu M. Capillary isoelectric focusing. Electrophoresis. 1997;18:2134-44.

[4] Righetti PG, Gelfi C, Conti M. Current trends in capillary isoelectric focusing of proteins. J Chromatogr B. 1997;699:91-104.

[5] Shimura K. Recent advances in capillary isoelectric focusing: 1997-2001. Electrophoresis. 2002;23:3847-57.

[6] Kilár F. Recent applications of capillary isoelectric focusing. Electrophoresis. 2003;24:3908-16.

[7] Shimura K. Recent advances in IEF in capillary tubes and microchips. Electrophoresis. 2009;30:11-28.

[8] Hühner J, Lämmerhofer M, Neusüß C. Capillary isoelectric focusing-mass spectrometry: Coupling strategies and applications. Electrophoresis. 2015;36:2670–86.

[9] Hjertén S, Zhu M. Adaptation of the equipment for high-performance electrophoresis to isoelectric focusing. J Chromatogr. 1985;346:265-70.

[10] Hjertén S, Liao J, Yao K. Theoretical and experimental study of high-performance electrophoretic mobilization of isoelectrically focused protein zones. J Chromatogr. 1987;387:127-38.

[11] Thormann W, Breadmore MC, Caslavska J, Mosher RA. Dynamic computer simulations of electrophoresis: a versatile research and teaching tool. Electrophoresis. 2010;31:726-54.

[12] Thormann W, Mosher RA. Instabilities of the pH gradient in carrier ampholyte-based isoelectric focusing: Elucidation of the contributing electrokinetic processes by computer simulation. Electrophoresis. 2021;42:814-33.

[13] Thormann W, Mosher RA. Dynamic computer simulations of electrophoresis: 2010-2020. Electrophoresis. 2022;43:10-36.

[14] Thormann W, Mosher RA. High-resolution computer simulation of electrophoretic mobilization in isoelectric focusing. Electrophoresis. 2008;29:1676-86.

[15] Thormann W, Mosher RA. High-resolution computer simulation of the dynamics of isoelectric focusing using carrier ampholytes: focusing with concurrent electrophoretic mobilization is an isotachophoretic process. Electrophoresis. 2006;27:968-83.

[16] Takácsi-Nagy A, Kilár F, Thormann W. The effect of pH adjusted electrolytes on capillary isoelectric focusing assessed by high-resolution dynamic computer simulation. Electrophoresis. 2022;43:669-78.

[17] Thormann W, Caslavska J, Mosher RA. Modeling of electroosmotic and electrophoretic mobilization in capillary and microchip isoelectric focusing. J Chromatogr A. 2007;1155:154-63.

[18] Thormann W, Zhang C-X, Caslavska J, Gebauer P, Mosher RA. Modeling of the impact of ionic strength on the electroosmotic flow in capillary electrophoresis with uniform and discontinuous buffer systems. Anal Chem. 1998;70:549-62.

[19] Hruška V, Jaroš M, Gaš B. Simul 5 - free dynamic simulator of electrophoresis. Electrophoresis. 2006;27;984-91.

[20] Tentori AM, Herr AE. Performance implications of chemical mobilization after microchannel IEF. Electrophoresis. 2014;35:1453-60.

[21] Hruška V, Gaš B, Vigh G. Simulation of desalting that occurs during isoelectric trapping separations. Electrophoresis. 2009;30:433-43.

[22] Gaš B, Bravenec P. Simul 6: A fast dynamic simulator of electromigration. Electrophoresis. 2021;42:1291-99.

[23] Bahga SS, Bercovici M, Santiago JG. Robust and high-resolution simulations of nonlinear electrokinetic processes in variable cross-section channels. Electrophoresis. 2012;33:3036-51.

[24] Chou Y, Yang R-J. Simulations of IEF in microchannel with variable cross-sectional area. Electrophoresis. 2009;30:819-30.

[25] Ansorge M, Gaš B, Boublík M, Malý M, Šteflová J, Hruška V, Vigh G. CE determination of the thermodynamic pK_a values and limiting ionic mobilities of 14 low molecular mass UV absorbing ampholytes for accurate characterization of the pH gradient in carrier ampholytes-based IEF and its numeric simulation. Electrophoresis. 2020;41:514-22.

[26] Mack S, Cruzado-Park I, Chapman J, Ratnayake C, Vigh G. A systematic study in CIEF: defining and optimizing experimental parameters critical to method reproducibility and robustness. Electrophoresis. 2009;30:4049-58.

[27] Bonn R, Rampai S, Rae T, Fishpaugh J. CIEF method optimization: development of robust and reproducible protein reagent characterization in the clinical immunodiagnostic industry. Electrophoresis. 2013;32:825-32.

[28] Kristl T, Stutz H. Comparison of different mobilization strategies for capillary isoelectric focusing of ovalbumin variants. J Sep Sci. 2015;38:148-56.

[29] Duša F, Moravcová D, Šlais K. Low-molecular-mass nitrophenol-based compounds suitable for the effective tracking of pH gradient in isoelectric focusing. Anal Chim Acta. 2019;1076:144-53.

[30] Wang L, Bo T, Zhang Z, Wang G, Tong W, Chen DDY. High Resolution capillary isoelectric focusing mass spectrometry analysis of peptides, proteins, and monoclonal antibodies with a flow-through microvial interface. Anal Chem. 2018;90:9495-503.

[31] Mack S, Arnold D, Bogdan G, Bousse L, Danan L, Dolnik V, et al. A novel microchip-based imaged CIEF-MS system for comprehensive characterization and identification of biopharmaceutical charge variants. Electrophoresis. 2019;40:3084-91.

[32] Zhu M, Rodriguez R, Wehr T. Optimizing separation parameters in capillary isoelectric focusing. J Chromatogr. 1991;559:479-88.

[33] Manabe T, Miyamoto H, Iwasaki A. Effects of catholytes on the mobilization of proteins after capillary isoelectric focusing. Electrophoresis. 1997;18:92-7.

Legends

Figure 1. Simulated IEF pattern with 14 analytes in a pH 3.0-10.3 gradient formed by 182 carrier ampholytes after focusing for 3000 s at a constant 100 V in a 50 µm id capillary of 54 mm length and having circular electrode compartments with (A) 5000 µm id and (B) 50 µm id. Analytes (0.01 mM each), carrier ampholytes (0.1 mM each), iminodiacetic acid (IDA, 10.5 mM) and arginine (ARG, 8.79 mM) were supplied as homogeneous mixture between 300 mM H_3PO_4 (anolyte, 0 to 9 mm of column length) and 200 mM LiOH (catholyte, 63 to 72 mm of column length). The distributions of all components, the foci of the 14 analytes between IDA (dark green line) and ARG (dark pink line), the electrolytes and spacing components, and pH, conductivity (red line) and electric field strength (broken line) are presented from bottom to top, respectively. The cathode is to the right. The inserts depict the current as function of time. Key: 1, serotonin (pI 10.58); 2, tyramine (10.17); 3, metanephrine (9.72); 4, epinephrine (9.32); 5, norepinephrine (9.21); 6, labetalol (8.49); 7, 3-methylhistidine (7.71); 8, glycyl-histidine (7.55); 9, leucoberbelin blue I dye (5.27); 10, 4-(4-aminophenyl) butyric acid (4.86); 11, dansylated γ-aminobutyric acid (4.20); 12, dansylated glutamic acid (3.49); 13, dansylated aspartic acid (3.34); 14, dansylated iminodiacetic acid (2.99).

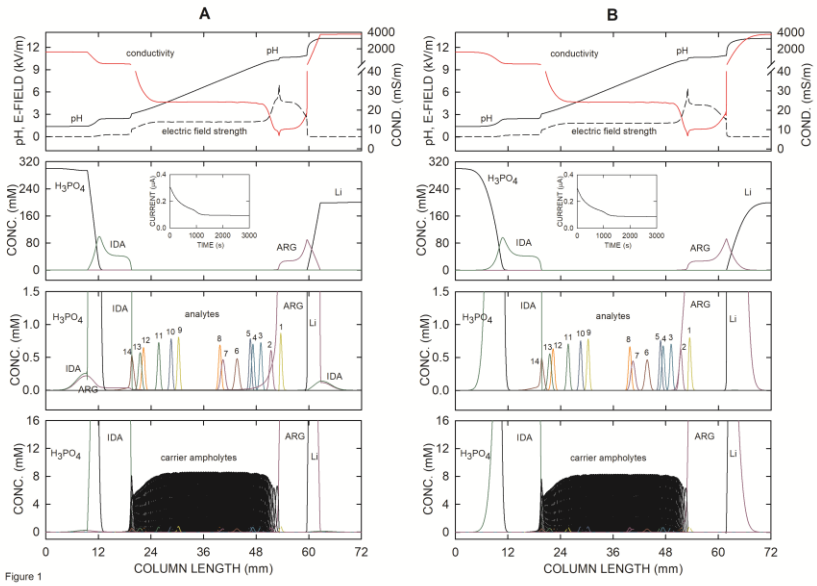

Figure 1

Figure 2. (A) Electrophoretic mobilization towards the cathode of the system of Figure 1A was induced by replacing the cathodic electrode solution with 300 mM phosphoric acid (bottom panel) and reapplication of a constant 100 V. Depicted distributions are those for 1000 s, 2000 s and 3000 s of mobilization (4000s, 5000 and 6000 s of total time, second, third and fourth panel form bottom, respectively). (B) Concentration profiles at a 100 s interval of migrating analytes with pI values of 3.49, 5.27, 7.55 and 9.21 (from bottom to top, respectively) and distributions of phosphoric acid, electric field strength and pH (at a 500 s interval each) between 3000 and 6000 s total time (up to 3000 s of mobilization). The dashed vertical lines demarcate the capillary ends (black lines) and the position of the detector (dark grey line). The numbers in panel B refer to the total time in seconds of the 2-step procedure.

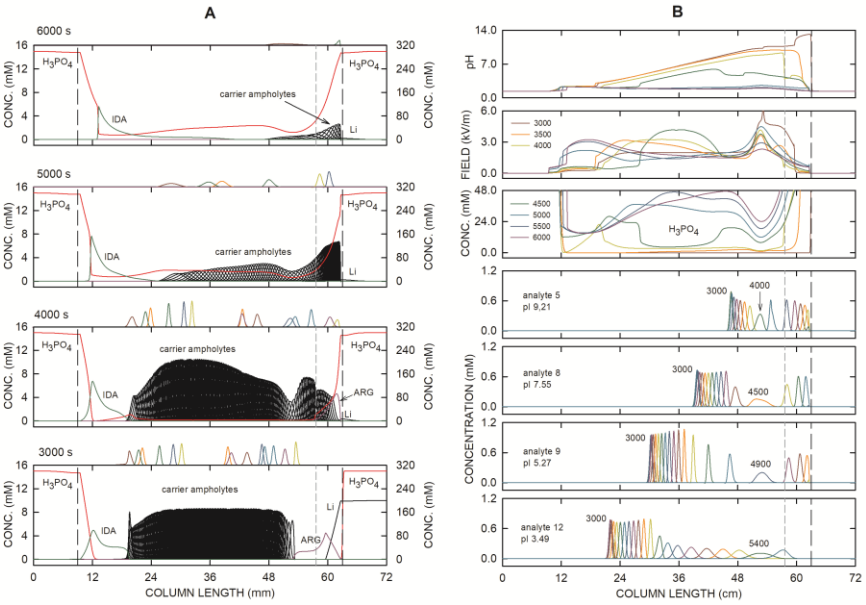

Figure 2

Figure 3. Computer predicted detector plots registered during mobilization for a detector placed at 57.6 mm featuring the responses of the analytes, ARG (dashed dark pink line, y-axis to the left) and the mobilizing compound (dashed dark grey line, y-axis to the right) for 300 mM catholytes composed of (A) phosphoric acid, (B) citric acid, (C) GLU, (D) chloroacetic acid, (E) formic acid, and (F) acetic acid. The upper panels comprise the corresponding pH (brown line) and conductivity detector signals together with the temporal behavior of the current (red line). Key as for Figure 1.

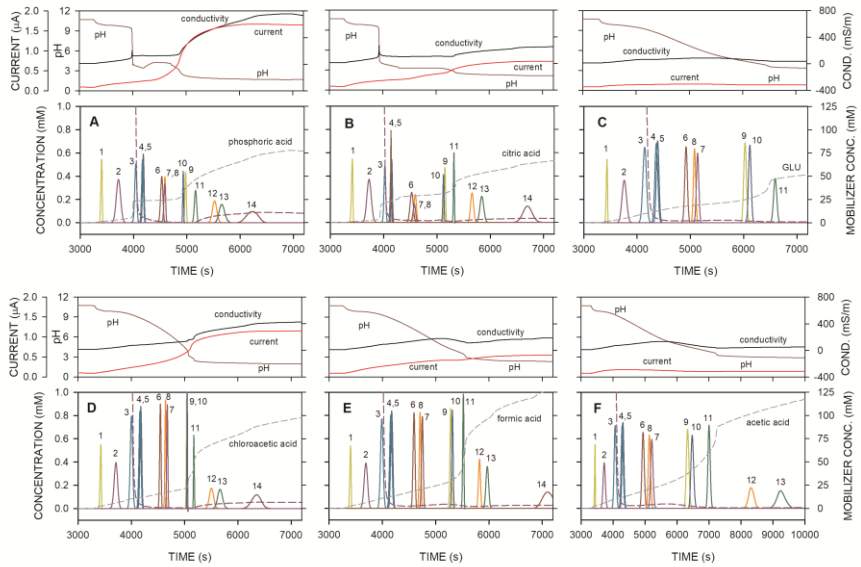

Figure 3

Figure 4. Mobilization data with (A) GLU and (B) formic acid. Depicted profiles represent those for the concentration of migrating analytes with pI values of 3.49, 5.27, 7.55 and 9.21 (from bottom to top, 100 s interval), as well as the mobilizing compound, the electric field strength and pH (at a 500 s interval each) between 3000 and 6000 s total time (up to 3000 s of mobilization). The dashed vertical lines demarcate the capillary ends (black lines) and the position of the detector (dark grey line).

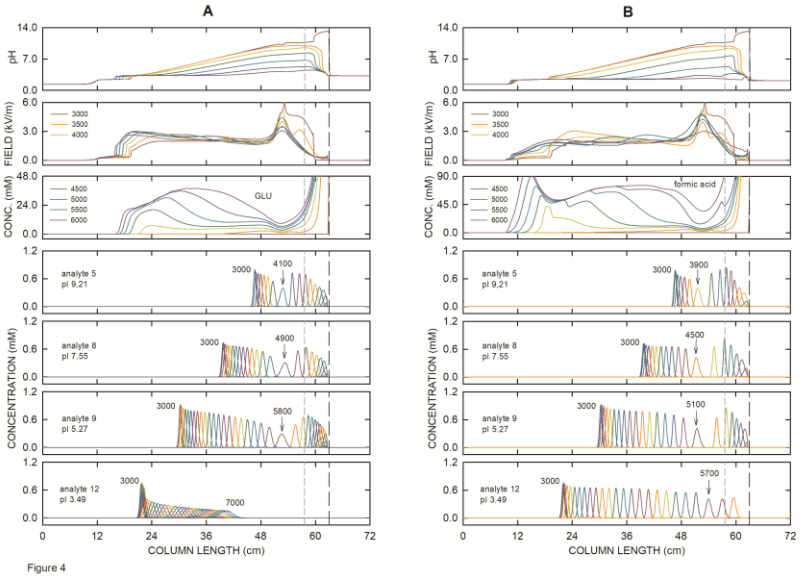

Figure 5. Data after focusing without ARG and IDA and otherwise identical conditions as for Figure 1A with (A) phosphoric acid and (B) formic acid as mobilizing compound. Depicted profiles represent those for the concentration of the migrating analyte with a pI 5.27 (bottom graphs, 100 s interval), as well as the mobilizing compound, the electric field strength and pH (at a 500 s interval each) between 3000 and 6000 s total time (up to 3000 s of mobilization). The dashed vertical lines demarcate the capillary ends (black lines) and the position of the detector (dark grey line).

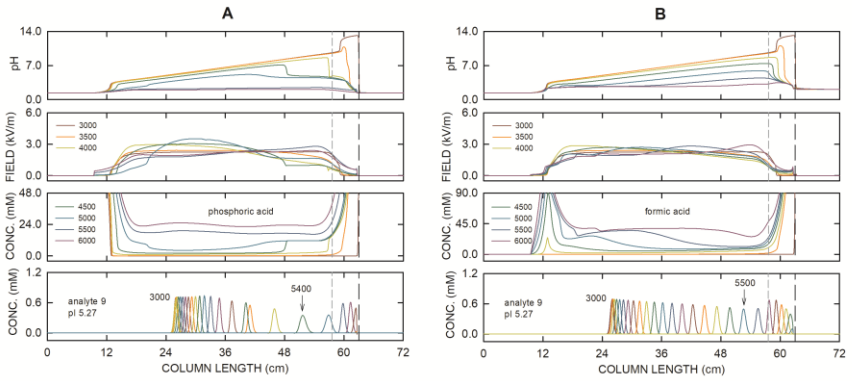

Figure 5